

Crystallization and Thermomechanical Properties of PLA Composites: Effects of Additive Types and Heat Treatment

J. Wootthikanokkhan,¹ T. Cheachun,¹ N. Sombatsompop,¹ S. Thumsorn,² N. Kaabbuathong,³ N. Wongta,¹ J. Wong-On,¹ S. Isarankura Na Ayutthaya,¹ A. Kositchaiyong¹

¹Division of Materials Technology, School of Energy, Environment, and Materials, King Mongkut's University of Technology Thonburi [KMUTT], Bangmod, Bangkok 10140, Thailand

²Rajamangala University of Technology Thanyaburi, Pathumthani 12110, Thailand

³PTT Research and Technology Institute, PTT Public Co. Ltd. Wang Noi, Ayutthaya, Thailand

Correspondence to: J. Wootthikanokkhan (E-mail: Jatuphorn.woo@kmutt.ac.th)

ABSTRACT: This research work has concerned a study on thermomechanical and crystallization properties of poly(lactic acid) (PLA) composites containing three different types of additives; namely: kenaf fiber (20 pph), Cloisite30B nanoclay (5 pph), and hexagonal boron nitrile (h-BN; 5 pph). The composites were prepared using a twin screw extruder before molding. Crystallization behaviors of the various composites were also examined using a differential scanning calorimetry. By adding the additives, tensile modulus of the polymer composites increased, whereas their tensile strength and elongation values decreased as compared to those of the neat PLA. Heat distortion temperature (HDT) values of the materials slightly increased, for about 3–5°C. However, after annealing at 100°C, HDT values of the fabricated PLA composites rapidly increased with annealing time before reaching a plateau after 10 min. The HDT values of above 120°C were achieved when 20 pph kenaf fiber was used as an additive. The above results were in a good agreement with DSC thermograms of the composites, indicating that percentage crystallinity of the materials increased on annealing and crystallization rate of the PLA/kenaf system was the highest. © 2012 Wiley Periodicals, Inc. *J. Appl. Polym. Sci.* 129: 215–223, 2013

KEYWORDS: polyesters; biodegradable; composites; nanostructured polymers

Received 18 July 2012; accepted 8 October 2012; published online 6 November 2012

DOI: 10.1002/app.38715

INTRODUCTION

Development of biobased plastic products for use as a replacement of petroleum-based plastics has been a subject of great interest for both academic and industry perspectives over the past decade. The above trends are driven by many factors including the run-out of oil reserve, the rise in oil price, and the effort to reduce pollutions attributed to CO₂ emission and plastic waste.¹ In this regard, poly(lactic acid) (PLA) is considered to be one of the most promising biobased materials for many applications such as food packaging² fibers for nonwovens, textiles and carpets,³ disposable cutlery, cup, containers, and housing for laptop computers and electronic devices.^{4,5} This is due to the fact that PLA has a high melting point, being commercially available, and biodegradable over the period of several months to 2 years.⁶ In addition, reduction of CO₂ emission as much as 85% of PLA has also been claimed.¹

Despite these desired features, considerable efforts have been made to cope with some disadvantage and/or limitations of PLA. These include the high brittleness of the polymer, low heat

distortion temperature (HDT) value (50°C) which are insufficient for some applications such as containers for hot drink, automobile components,⁴ and electronic products.⁵ In this regard, thermomechanical properties of PLA have yet to be enhanced before using. One possible strategy for enhancing mechanical properties and HDT of polymers is to induce higher degree of crystallinity of the polymer. To promote a faster crystallization rate and a greater degree of crystallinity of PLA, certain additives capable of acting as a nucleating agent should be introduced into the polymer. These include nanoclays,^{7–11} natural fibers,^{12–14} and inorganic compounds such as hexagonal boron nitrile (h-BN).¹⁵

Capability of nanoclay as a nucleating for PLA has been demonstrated by Denualt et al.¹⁰ in a study on the effect of three different types of nanoclay, namely CloisiteNa, Cloisite20A, Cloisite30B, on thermal properties of PLA. It was found that the use of Cloisite30B (2 wt %) was the best additive system in terms of exfoliation and compatibilization, whereas, the use of CloisiteNa (2 wt %) led to the composite with the maximum

degree of crystallinity obtained. Similarly, Solarski et al.⁷ reported that by adding the Cloisite30B nanoclay, percentage crystallinity and thermal stability of PLA increased.

Mechanical properties of polymer nanocomposites are also dependent on the nanoclay loading. In general, tensile strength and modulus of polymer nanocomposites increased with clay loading at the expense of percentage elongation and toughness of the materials. For PLA nanocomposite, the optimum clay content of 5 pph, with respect to the mechanical properties improvement, was used.¹¹ Similarly, the optimum clay content with respect to thermomechanical properties of the PLA nanocomposites ranged between 4 and 7 pph.⁹ Specifically, HDT value of the PLA nanocomposites, containing an organo-montmorillonite (MMT), increased from 76 to 94 and 112°C after adding 4 and 7% of the nanoclay, respectively.

Alternatively, some natural fibers might be used to enhance mechanical properties, crystallinity, and HDT of PLA. In this regard, the length and content of the fiber are important factors affecting mechanical properties of polymer composite. For example, work by Ahmad et al.¹⁶ found that flexural strength and impact strength of poly(butylene succinate)/kenaf fiber composites initially increased and then decreased with the fiber length. The optimum fiber length corresponding the maximum flexural strength is 10 mm. Noteworthy, it was found that the fiber length degradation occurred after compounding, regardless of the initial fiber length. It was also found that flexural strength of the composites increased with the fiber content at the expense of their impact strength. The optimum fiber content was 20 pph, beyond which the mechanical properties did not significantly change. The results were discussed in relation to agglomerations between the neighboring fibers and thus weakened the composite. Similarly, Garcia et al.¹⁷ studied PLA/kenaf fiber composites and found that impact strength of the materials decreased on an incorporation of 20 pph of the fiber. Beyond this level, the impact strength was not significantly different. Ochi¹⁸ also investigated mechanical properties and biodegradability of PLA/kenaf fiber composites and found that tensile strength, flexural strength, and elastic modulus of the kenaf fiber-reinforced PLA composites increased linearly up to a fiber volume fraction of 50%. Serizawa et al.^{12,13} studied thermomechanical properties of PLA composites containing 10–30 pph of a short kenaf fiber (3 mm long). It was found that HDT value of PLA increased from 66 to 120°C, at the expense of impact strength and flexural strength, after adding 20 pph of the fiber. It is worth mentioning that the specimen annealed at 100°C for 4 h before testing could induce an increased crystallinity of the PLA. Work by Ibrahim et al.¹⁴ showed that by using triacetin as a plasticizer for PLA compounding, HDT value of the PLA/kenaf composite system dropped. It was because the presence of triacetin plasticizer increased the free volume of PLA and restricted nucleation and crystallization of the polymer.

To ensure dimension stability of PLA products for some packaging applications such as hot boiling water containers, it seems that HDT value of the PLA composites has yet to be further enhanced. Unfortunately, from the literature reviews, HDT of the annealed PLA compounds at above 120°C have not been reached and/or reported elsewhere. Besides, the annealing time

reported^{9,12,13} and used in the literature was considerably long (such as for 4 h at 100°C or 30 min at 120°C). To minimize the annealing time and to achieve the HDT value of greater than 120°C, crystallization behaviors and a suitable type of additive to be used for enhancing crystallinity of PLA have yet to be further investigated and identified. In this study, PLA composites containing three different additives, namely kenaf fiber, nanoclay (Cloisite30B), and h-BN are of interest. The aim of this work is to investigate the effect of additive types and annealing time on percentage crystallinity, crystallization rate, HDT, and tensile properties of the PLA compounds.

EXPERIMENTAL

Chemicals

PLA (3051D from NatureWork) was supplied from the Fresh Bag Co. Ltd. Kenaf fiber (grade 3MM) was supplied by Engauge Resources (Bangkok, Thailand) Co. Ltd. Average length and average diameter of the as received fiber, determined by using an optical microscopy, are 7.23 mm and 90 μm , respectively. The fiber length was further reduced to an average value of 1.37 mm before use. This was to avoid entanglement of the fiber during mixing which caused some problems with fiber dispersion and process-ability. Apart from this, the fiber was used as received without any further surface pretreatment. Cloisite30B nanoclay, which is a kind of organo-MMT modified with methyl, hydrogenated tallow, bis-2-hydroxyl, quaternary ammonium, was supplied from Southern Clay Product, Inc (TX, USA). Average particle size of the nanoclay range between < 13 μm (90%) and < 2 μm (10%). h-BN with the actual averaged particle size of 1.5 μm , was purchased from M K Impex (Ontario, Canada).

Preparation of PLA Compounds

PLA pellet was dried in a vacuum oven at 80°C for 2 h. After that, the dried polymer pellets were premixed with the additives (namely kenaf fiber, Cloisite30B, and h-BN in a high speed mixer (Labtech Engineering, Samutprakarn, Thailand), at an ambient temperature. Noteworthy, the amounts of additives used for compounding with PLA were different, ranging from 20 pph for the kenaf fiber and 5 pph for Cloisite30B and h-BN, respectively. These amounts were selected on the basis of the optimum values reported in literature.^{7,9–13,15–17} After premixing, the mixture was fed through a hopper of a twin screw extruder (Thermo Scientific Haake, PolyLab QC machine, Karlsruhe, Germany), equipped with a strand die and operated at a screw rotating speed of 100 rpm. The temperature profiles used from the extruder feed through the die zones were 120, 140, 160, 170, and 160°C, respectively. The extrudate was then cooled in a water-bath before undergoing a pelletization process to obtain composite granules.

Fabrication

PLA extrudates containing different types of additives were fabricated into 185 \times 185 mm² rectangular test pieces by using a 0.5-mm thick mold in a hydraulic compression molding machine (Labtech Engineering, Model T16, Samutprakarn, Thailand). The samples were preheated at 160°C for 2 min before compression molded at the temperature of 170°C under a mold pressure of 150 kg/cm³ for 3 min. After that, the fabricated sample was allowed to cool in the mold for 5 min before

demolding. For HDT test, the extrudate was fabricated into 127×127 mm² rectangular test pieces by using a 4.0-mm thick mold, using the same compression molding machine and conditions. Additionally, to study the effect of annealing time on thermomechanical properties of PLA/kenaf fiber composite, the extrudate was fabricated using an injection molding machine (Battenfeld, HM 65/210s, Kottlingbrunn, Austria), at 175°C, 1250 bar, and 50 cm²/s. The mold temperature was 31°C, whereas the holding time and cooling time used were 13 and 25 s, respectively.

Thermal Analysis

Thermal behaviors of the various PLA composites were examined using differential scanning calorimetry (DSC) technique. The experiment was conducted using a Perkin–Elmer equipment (DSC 8000 model, Waltham, MA), under nitrogen gas atmosphere. The sample was scanned, at a heating rate of 10°C/min, over temperatures ranging between 20 and 200°C and maintained at 200°C for 2 min. After that, the sample was slowly cool down to 20°C at 10°C/min, and maintained at that temperature for 2 min, before the second DSC heating. From DSC thermograms, degree of crystallinity of the PLA was determined using the following equation;

$$\text{Crystallinity}(\%) = \frac{(\Delta H_m - \Delta H_c) \times 100}{\Delta H_{f100} \times (W_p)} \quad (1)$$

where ΔH_m = enthalpy of melting (J/g), ΔH_c = enthalpy of cold crystallization (J/g), ΔH_{f100} = enthalpy of melting for 100% crystalline PLA (93.0 J/g), and W_p = weight fraction of PLA in the composite materials.

Isothermal crystallization of PLA compounds were also studied by heating all of the PLA and PLA composite samples from 25 to 190°C at a DSC scanning rate of 10°C/min. After that, the samples were kept at 190°C for 3 min to destroy their thermal history. Then, the samples were cooled to a crystallization temperature (100°C), at the rate of 30°C/min and the isothermal crystallization was studied for 30 min. From the isothermal DSC thermogram, rate of crystallization and related parameters were calculated using an Avrami's eqs. (2) and (3)

$$X(t) = 1 - \exp(-kt^n) \quad (2)$$

$$K = \frac{\ln 2}{(t_{1/2})^n} \quad (3)$$

where $X(t)$ = relative crystallinity, k = crystallization rate constant (min⁻ⁿ), n = Avrami exponent, t = time (min), and $t_{1/2}$ = half time crystallization (min).

Mechanical Properties Test

Mechanical properties of the various composites were evaluated via tensile test. Dumbbell-shaped specimens were prepared by cutting the fabricated PLA compound sheets to comply with an ASTM D638 standard test method. The tensile test was carried out using a LLOYD instrument (LR 50K model, Fareham Hants, UK) at a crosshead speed of 100 mm/min at room temperature. At least five specimens were tested for each run. Average values of the Young's modulus, tensile strength at break, and elongation at break were then calculated and reported. In addition,

toughness values of the blends were obtained by calculating the area under the force-displacement curves from the tensile test.

Additionally, HDT under 0.455 MPa load of the various PLA composites were determined using a Wallace Plastometer (Surrey, England), in accordance with ASTM D 648-01 Method, B. The test pieces of $4 \times 12.7 \times 127$ mm³ were heated at a rate of 2°C/min in silicone oil bath, and the temperature when the test piece has deflected at 0.25 mm was reported as HDT value.

Scanning Electron Microscopy

Morphology of the PLA compounds were examined using scanning electron microscopy (SEM) technique. The SEM specimen was prepared by cryogenic fracturing of the rectangular test-pieces under liquid nitrogen. After that, the fractured surfaces were coated with Au, using a gold sputtering technique (SPI-module™ coater, S/N 10081 MODEL) before SEM experiment. This was to avoid a charging effect during the electron beam scanning. The SEM experiment was operated using a JEOL machine (JSM5800, Tokyo, Japan), equipped with a secondary electron detector under an accelerating voltage of 10 kV.

Intercalation and exfoliation of nanoclay in the nanocomposites were investigated with an X-ray diffraction (XRD) technique with a diffractometer (D8-Discover model from Bruker AXS, Madison, WI). The operation was in the γ - γ geometry. The instrument used radiation from a copper target tube (Cu K α radiation wavelength 1.5406 Å). The XRD data were collected between 2 and 60° in a step size of 0.02 degree/step, with an X-ray generator.

Infrared Spectroscopy

The Fourier transform infrared (FTIR) experiment was carried out in an attenuated FTIR (reflection) mode, using a Thermo instrument (iS 5 model). The samples were scanned over wavenumbers ranging between 500 and 4000 cm⁻¹.

RESULTS AND DISCUSSION

Crystallinity

Figure 1 shows DSC thermograms of fabricated PLA and the PLA composites containing different types of additives. An endothermic enthalpy changes occurred at the temperature of around 55–60°C and that could be ascribed to a glass transition temperature of PLA. A small crystallization melting peak of the PLA at 150°C was also noted, indicating that the cooling time in the mold was not sufficiently long for PLA to be completely crystallized. This was not the case when the neat PLA pellets are considered. In this regard, DSC thermogram (Figure 2) of the specimen shows a large endothermic crystalline melting peak at 150°C, corresponding to the percentage crystallinity value of 39.6%. The discrepancy was ascribed to the different thermal history between the neat PLA pellets and the PLA sheet, fabricated via a compression molding.

From the Figure 1, it was also found that additional peaks immersed after adding the additives to PLA. For the PLA/kenaf composite, a broad exothermic peak located at the temperature ranging between 110 and 140°C was noted. This could be ascribed to some crystallization of the polymer during DSC scanning. For the PLA/Cloisite30B and PLA/h-BN composites,

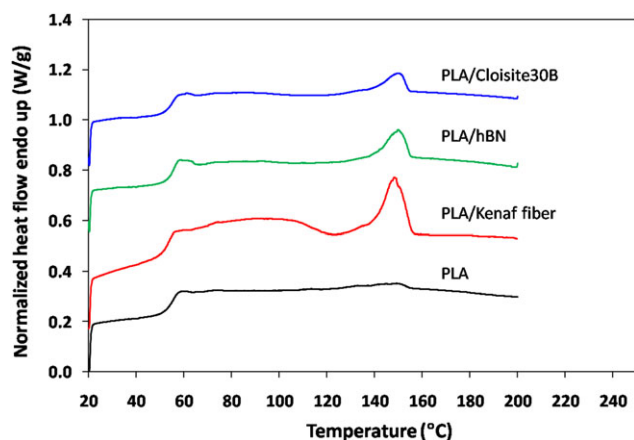


Figure 1. DSC thermograms of fabricated PLA and PLA composites, obtained from the first heating. [Color figure can be viewed in the online issue, which is available at wileyonlinelibrary.com.]

however, magnitudes of the exothermic peaks became less obvious. It is apparent that the crystallization rates of these composites are lower than that of the PLA/kenaf system. In addition, a large endothermic peak at 150°C can be obviously seen from DSC thermograms of the composites. This can be referred to as a melting peak of the bulk PLA phase. In this regard, by using the eq. (1), the actual percentage crystallinity of various fabricated PLA composites (before DSC analysis) were calculated and reported in Table I. It can be seen that percentage crystallinity of the polymer hardly increased with adding the various additives. This effect is different from those were reported by Serizawa et al.¹² and Ray et al.⁸ in a study on PLA/kenaf fiber and PLA nanocomposite, respectively. Specifically, in the latter case, percentage crystallinity of PLA increased from 36 to 46% after adding 7 pph of organically modified synthetic fluorine silica. A possible explanation for the discrepancy between this work and the literature^{8,11} includes the fact that the PLA composites in this study have not been annealed, whereas those from the literature experienced some heat treatment before the DSC experiment. As a result, thermal history and degree of crystallinity were different.

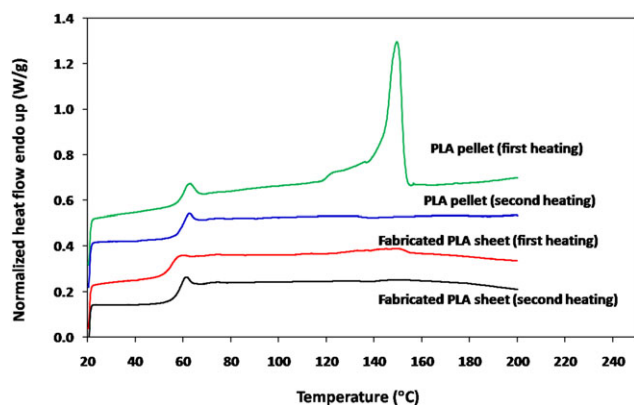


Figure 2. DSC thermograms of PLA resins and the fabricated PLA sheets obtained from the first and the second heating. [Color figure can be viewed in the online issue, which is available at wileyonlinelibrary.com.]

Table I. Percentage Crystallinity of PLA Composites before Annealing

Samples	Crystallinity (%)	
	First DSC scan	Second DSC scan
PLA	3.2	-
PLA/kenaf fiber	7.5	3.0
PLA/h-BN	8.1	2.1
PLA/Cloisite30B	2.4	2.7

Attempts were also made to investigate second heating DSC thermograms of the neat PLA pellets (Figure 2). After the first heating DSC experiment, the samples were slowly cooled at 10°C/min before reheating. It was found that the melting peak of PLA disappeared and percentage crystallinity of the polymer dropped (Table I). Again, this implies that PLA could not be recrystallized under the above cooling rate. To further enhancing crystallinity of the polymer, the samples should be annealed. In this regard, the effects of annealing conditions on thermomechanical properties of PLA compounds deserve a consideration.

Figure 3 shows DSC thermograms of fabricated PLA and the related composites after annealing in an oven at 100°C for 4 h. Percentage crystallinity of the annealed PLA remarkably increased (Table II). Furthermore, the use of additives is also capable of further enhancing percentage crystallinity of the annealed PLA slightly. This can be related to the presence of an additional PLA melting peak on the left at 142°C. Similar DSC behavior was also observed by Praprudivongs et al.¹⁹ and Shi et al.²⁰ in the studies on PLA/wood composite and PLA/bamboo-fiber/talc composite, respectively. In this study, it was believed that the presence of additives causes imperfections of PLA crystals. On annealing, transcrystallization process of PLA at the polymer-additives interface might occur to form perfect and stable crystal.²¹ The above notion was also supported by considering the results from isothermal DSC thermograms of the composites, which was described in the subsequent section.

Mechanical Properties

Figures 4–6 show tensile properties of PLA compounds. After mixing with the additives, tensile modulus of PLA increased

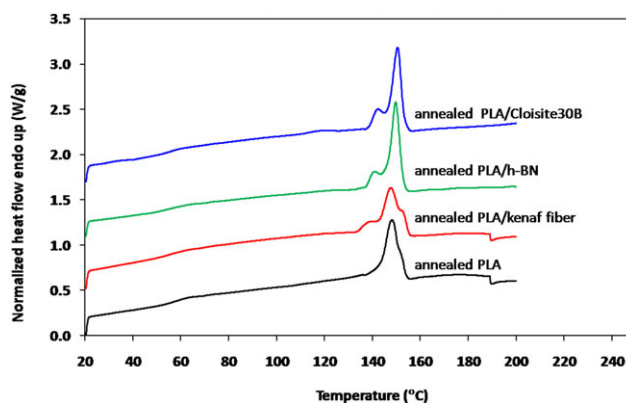


Figure 3. DSC thermograms of PLA and PLA composites after annealing at 100°C for 4 h (first heating). [Color figure can be viewed in the online issue, which is available at wileyonlinelibrary.com.]

Table II. Percentage Crystallinity of PLA and PLA Composites after Annealing

Samples	Crystallinity (%)	
	First DSC scan	Second DSC scan
PLA	33.9	-
PLA/kenaf fiber	37.4	1.1
PLA/h-BN	39.0	2.1
PLA/Cloisite30B	36.7	0.3

with decreases in tensile strength, and elongation. The tensile properties of PLA/kenaf fiber composite are the lowest as compared to those of the PLA composites containing Cloisite30B and/or h-BN, even though the value are comparable with that studied and reported by Srebrenkoska et al.²² on the similar PLA composite system. The above effects might be related to different compatibility levels between PLA and the various additives. For the PLA/kenaf composite, SEM images of the material (Figure 7) show some traces of pull-out fibers on the fractured surface. In this regard, it seems that an interfacial adhesion between PLA and kenaf fiber herein has yet to be further enhanced, even though polar interaction between ester functional groups of PLA and hydroxyl functional groups on the fiber surface is expected. In this regard, it was recommended that a silane coupling agent²³ and/or PLA-g-MA compatibilizer^{22,24} might be used to enhance the interfacial adhesion and tensile strength of the composites.

On the other hand, PLA seems to be compatible with Cloisite30B and h-BN. The compatibility between Cloisite30B and PLA can be attributed to a polar interaction between the carbonyl functional groups of PLA chains and hydroxyl functional groups of the alkyl ammonium surfactant, which was used to modify the clay. Besides, dispersion of the nanoclay within the polymer matrix also plays roles. Figure 7 shows XRD patterns Cloisite30B and PLA/Cloisite30B. The peak at 4.74° corresponding to interlayer distance ($d_{001} = 1.86$ nm) of the Cloisite30B nanoclay²⁵ can be seen from the XRD pattern of the clay. After mixing the nanoclay with PLA, the peak corresponding to d_{001} spacing of Cloisite30B was not clearly observed. This result implies that some exfoliation of Cloisite30B in the polymer matrix has occurred. This structure might contribute to the tensile modulus of the nanocomposite. The above discussions are in a good agreement with the results from a study on PLA nanocomposites by Nam et al.,²⁶ which found that dispersion of Cloisite30B in PLA matrix is better than that of other types of nanoclay.

For the PLA/h-BN composite system, FTIR spectra of h-BN and the polymer composite (Figure 8) show the characteristic strong absorption band at 1360 cm^{-1} , corresponding to the in plane B—N stretching vibration, along with the sharper peak at 774 cm^{-1} , attributing to the out of plane B—N—B bending vibration. In addition, the peak at 1748 cm^{-1} , representing C=O bond stretching vibration of the PLA molecules is also evidenced from the spectra of PLA and PLA/h-BN. In this regard, polar interaction between nitrogen's lone pair of electrons on

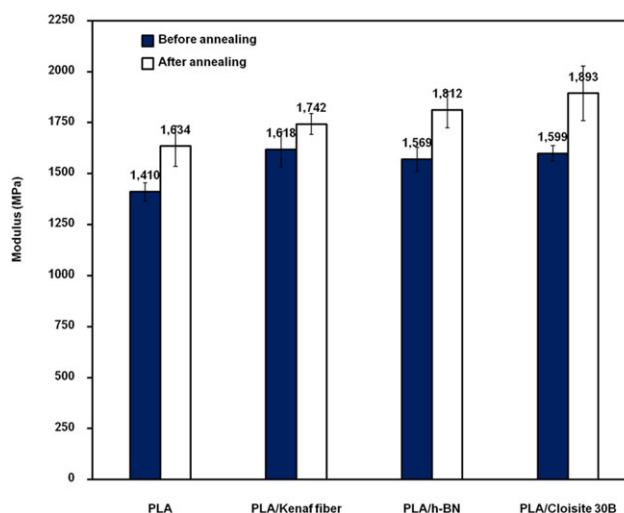


Figure 4. Tensile modulus of various PLA composites. [Color figure can be viewed in the online issue, which is available at wileyonlinelibrary.com.]

the surface of h-BN and the carbonyl functional groups of PLA can be expected.²⁷ This interaction might contribute to a better tensile strength of the composite, as compared to that of the PLA/kenaf composite system. Consideration of an XRD pattern of the PLA/h-BN composite (Figure 9), however, reveals that the peak at 28°, corresponding to the inter layer distance of 0.334 nm of the h-BN, was remained after mixing with PLA. This implies that an intercalation structure or an insertion of polymer into the layers of h-BN was not achieved. This was in a good agreement with both experiment and theory, suggested the intercalation for boron nitrile is difficult.²⁸

Nevertheless, a good interfacial adhesion between PLA and the additives as well as the superior tensile strength of the two composites (PLA/Cloisite30B and PLA/h-BN) were supported by the SEM images of the materials (Figure 10). It can be seen that the specimen's surface lack of phase separation, poor interface, and

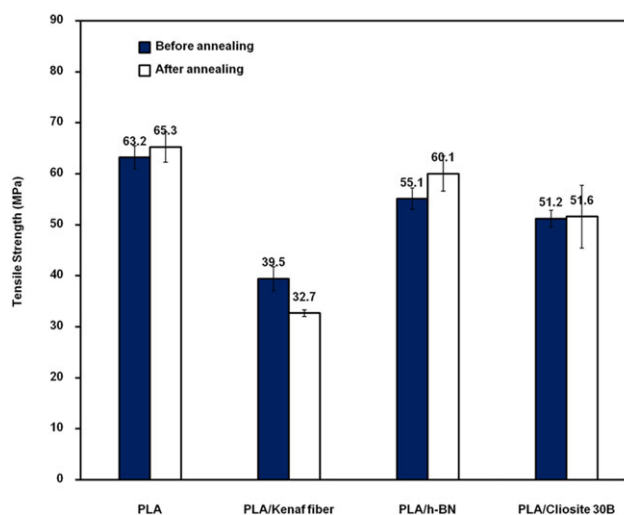


Figure 5. Tensile strength of various PLA composites. [Color figure can be viewed in the online issue, which is available at wileyonlinelibrary.com.]

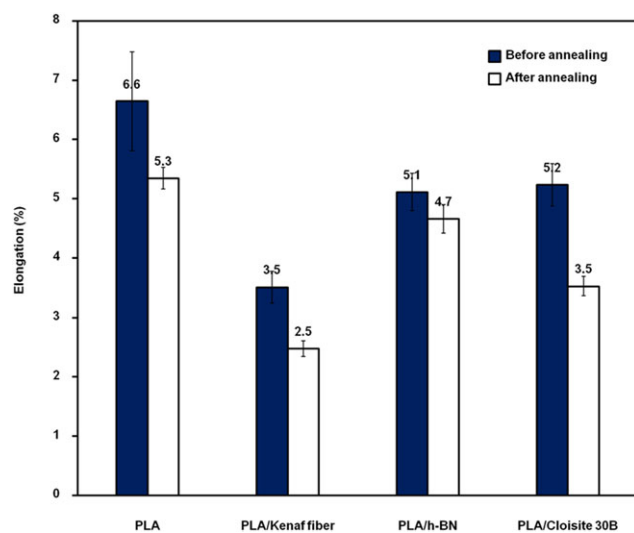


Figure 6. Elongation of various PLA composites. [Color figure can be viewed in the online issue, which is available at wileyonlinelibrary.com.]

agglomeration h-BN at the micrometer scale. Besides, fracture surfaces of the composites are also rougher as compared to that of the neat PLA surface. This feature reflects a kind of plastic deformation and not brittle fracturing of the composites.

Effects of Annealing on Thermomechanical Properties

After annealing in an oven at 100°C for 4 h, tensile properties of the PLA composites hardly changed (Figures 4–6). However, thermomechanical properties of PLA and PLA composites improved significantly. Figure 11 shows that HDT value of the

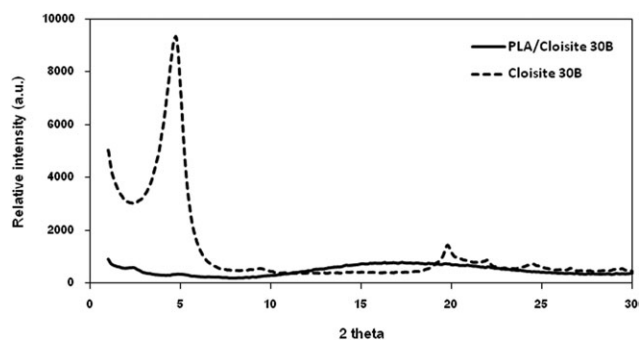


Figure 7. XRD patterns of Cloisite30B and PLA/Cloisite30B composite.

neat PLA specimen rapidly increased from 53.2 to 99.7°C after annealing. In addition, the HDT values of the annealed PLA composites were also slightly greater than that of the annealed neat PLA. From this study, the highest HDT value is 128°C, which was obtained by annealing PLA/kenaf fiber (20 pph) composite. To the best of our knowledge, this is the highest HDT value, compared with those reported in the open literature.^{12,17} Next, the second highest HDT value (111°C) was obtained from the annealed PLA/h-BN specimen. The use of Cloisite30B as an additive for PLA also led to an increase in HDT value of the polymer from 57 to 103°C after annealing. The latter value is also comparable to that reported by Ray et al.⁹ in a study on HDT of annealed PLA nanocomposite, using organo-MMT modified with trimethyl-octadecylammonium cation.

In our opinion, these improvements were caused by two possible factors, that is, changes in percentage crystallinity of PLA

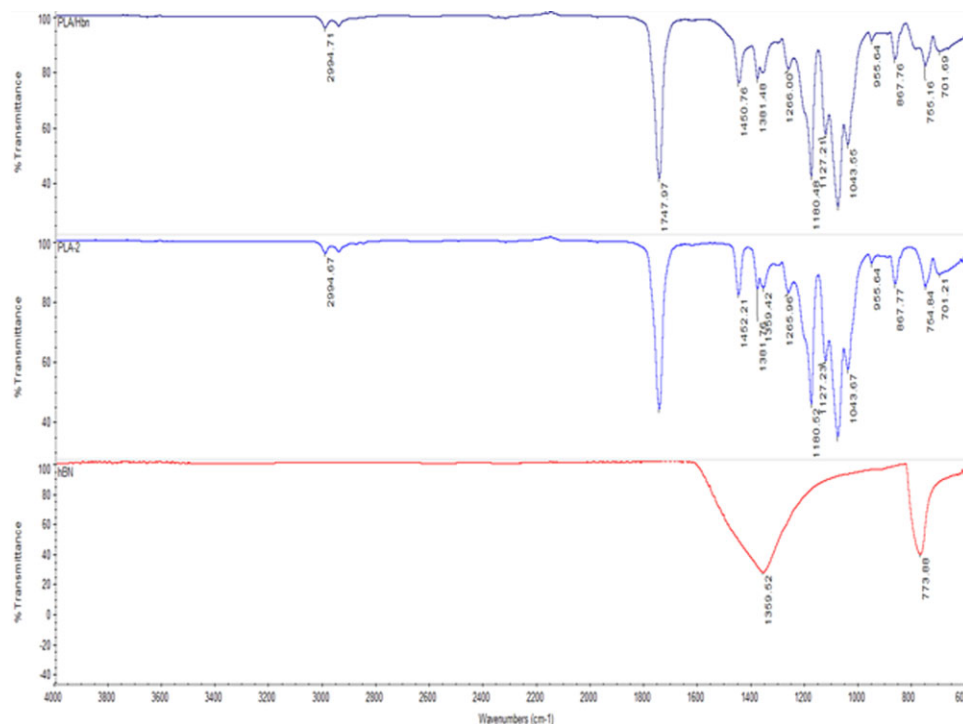


Figure 8. ATR-FTIR spectra of hexagonal boron nitride (h-BN) and PLA/h-BN composites. [Color figure can be viewed in the online issue, which is available at wileyonlinelibrary.com.]

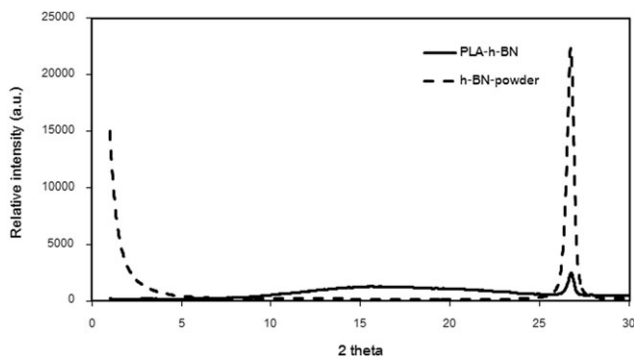


Figure 9. XRD patterns of hexagonal boron nitrile (h-BN) and PLA/h-BN composites.

phase induced by annealing (Tables I and II) and the different capability of the additives for reinforcing PLA. Particularly, the latter effect is related to different dimensions (size) of the three additives. The kenaf is a kind of fibrous material, with the averaged length and diameter of 1.37 mm and 90 μm , respectively. These correspond to an aspect ratio of 15. On the other hand, averaged particle sizes of Cloisite30B and h-BN were 13 and 5 μm , respectively.^{29,30} In this regard, the longer the fiber length the greater the reinforcing efficacy. This is due to the fact that an external applied load has to be transferred from the fiber to the polymer matrix and the greatest stiffness occurs when the

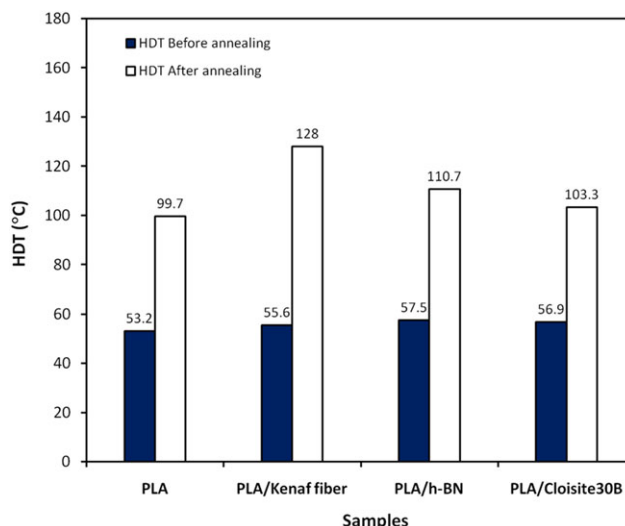


Figure 11. Heat distortion temperature (HDT) of various PLA composites both before and after annealing. [Color figure can be viewed in the online issue, which is available at wileyonlinelibrary.com.]

fibers are sufficiently long, compared with their diameter. For short-fiber composite, the fiber aspect ratio of at least 100–200 is required³¹ to achieve a longitudinal modulus approaching that of a continuous fiber composite. In practice, however, the fibers are usually of the order of a few millimeters in length.^{5,32}

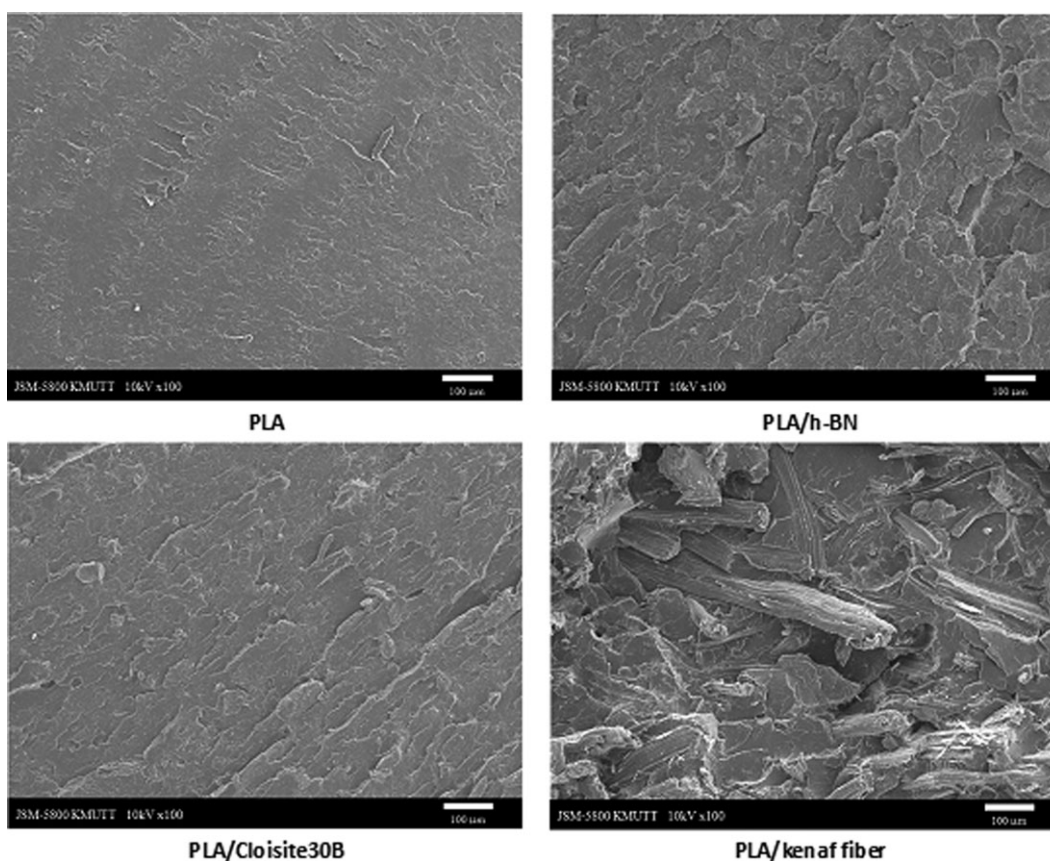


Figure 10. SEM micrographs of various PLA composites.

Table III. Percentage Crystallinity and HDT Values of PLA/kenaf Fiber Composites after Annealing at 100°C for Different Time

Annealing time (min)	Crystallinity (%)	HDT (°C)
0	7.5	55.7 (± 0.57)
10	32.5	123.0 (± 3.60)
20	32.1	127.7 (± 4.72)
240	29.6	128.0 (± 0.00)

This enable the composite to be processed easily using, for example, an injection molding.

From the HDT results, it seems that the PLA composite containing 20 pph kenaf fiber is the best formulation, provided that the fabricated composite specimen was annealed in an oven for 60 min before testing and use. In practice, however, the aforementioned time is considered relatively long with respect to a cycle time for producing some finished products, such as plastic cups, via an injection molding. Therefore, further attempts were made to investigate the effect of annealing time on thermomechanical properties of the composite. In this regard, the specimens, fabricated via an injection molding were annealed in an oven at 100°C for different periods of time. After that, changes in HDT values and mechanical properties were followed. From Table III, it was found that percentage crystallinity of the PLA/kenaf fiber composites rapidly increased from 7.5 to 32.0% after annealing for 10 min. Consequently, HDT value of PLA/kenaf fiber composite increased to above 120°C. By further increase the annealing time to 240 min, the HDT value only slightly increased from 123 to 128°C. These results are in a good agreement with the isothermal DSC thermograms of various PLA composites (Figure 12), showing that the neat PLA did not crystallize at this temperature within the time frame of isothermal DSC scanning (30 min). On the other hand, by mixing with the kenaf fiber, the isothermal crystallization of PLA completed. Percentage crystallinity of the PLA/kenaf fiber calculated from the isothermal DSC thermogram is 26.5%. The value is lower than that reported in Table II (37.4%) for the annealed PLA/kenaf fiber specimen, which was obtained from a nonisothermal DSC experiment. The discrepancy could be attributed to the different annealing times used.

From the melting peak, crystallization rate constant (k), and the half-time crystallization ($t_{1/2}$) of the composite calculated by using the Avrami equation are 1.82×10^{-4} (min^{-n}) and 16.2 (min), respectively. For a comparison purpose, Liao et al.³³ studied crystallization kinetic of PLA containing different nucleating agents namely BaSO₄, CaCO₃, and TiO₂, and found that the crystallization rates at 120°C are 4.79×10^{-5} , 7.47×10^{-5} , and 8.54×10^{-5} min^{-n} , respectively. In relation to this work, it is apparently that the crystallization rate of PLA/kenaf is higher, taking into account the lower isothermal temperature that was used herein. Noteworthy, by replacing kenaf fiber with h-BN and Cloisite30B, the maximum of the isothermal DSC curves of the composites tended to shift to right along the time axis, respectively. This implies that the use of Cloisite30B and h-BN were also capable of inducing some crystallizations of the PLA for any given conditions. It is also apparently that the crystalli-

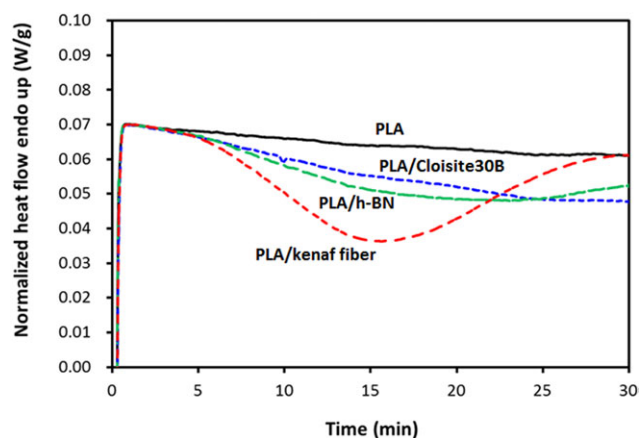


Figure 12. DSC thermograms of PLA composites under an isothermal condition. [Color figure can be viewed in the online issue, which is available at wileyonlinelibrary.com.]

zation rates of these composites are lower than that of PLA/kenaf. The crystallization rates of PLA/Cloisite30B, and PLA/h-BN systems are, however, not available due to the fact that the crystallization isotherms were not completed within the time frame of isothermal DSC scanning (30 min).

CONCLUSIONS

Effects of annealing on thermomechanical properties of PLA and PLA composites, containing three different additives, namely kenaf fiber, Cloisite30B nanoclay, and h-BN were investigated. HDT of PLA was improved after annealing and that can be related to the increase in percentage crystallinity of the polymer. In this study, the highest HDT value (128°C) was obtained when 20 pph of the kenaf fiber was mixed with the PLA, followed by annealing at 100°C for 60 min. By decreasing the annealing time to 10 min, the HDT value reduced to 123°C. The use of Cloisite30B and h-BN resulted in the composites with the relatively low HDT values, even though their tensile strength and percentage elongation were greater. Different effects of the various additives were related to the different crystallization rate of the relevant composites, supported by the isothermal DSC thermograms. Mechanical properties of the composites were also discussed in light of different aspect ratios and states of compatibility between PLA and the three additives, supported by the FTIR and XRD results.

ACKNOWLEDGMENTS

Dr. J Wootthikanokkhan and his colleagues at KMUTT are sincerely grateful to the PTT Research and Technology Institute for the financial support (TOR NO. 40004275). This work was also partly supported by the Higher Education Research Promotion and National Research University Project of Thailand, Office of the Higher Education Commission (Project No.277).

REFERENCES

1. Kawamoto, H. *Sci. Technol. Trends* **2007**, *22*, 62.
2. Weber, C. J.; Haugaard, V.; Festersen R.; Bertelsen G. J. *Food Addit. Contam.* **2002**, *19*, 172.

3. Siebott, V. PLA—the future of rigid packaging?; *Bioplastics Magazine* **2007**; Issue 1, pp 28–29.
4. Harris, A.M.; Lee, E.C. 6th Annual SPE Automotive Composites Conference, Troy, MI, 2006. Available at http://www.speautomotive.com/SPEA_CD/SPEA2006/PDF/c1.pdf. (accessed April, 2012).
5. Serizawa, S.; Inoue, K.; Iji, M. *J. Appl. Polym. Sci.* **2008**, *100*, 618.
6. Avella, M.; Buzarovska, A.; Errico, M. E.; Gentile, G.; Grozdanov, A. *Materials* **2009**, *2*, 911.
7. SolarSKI, S.; Mahjoubi, F.; Ferreira, M.; Devaux, E.; Bachelet, P.; Bourbigot, S.; Delobel, R.; Coszach, P.; Murariu, M.; Da Silva Ferreira, A.; Alexandre, M.; Degee, P.; Dubois, P. *J. Mater. Sci.* **2007**, *42*, 5105.
8. Sinha Ray, S.; Yamada, K.; Okamoto, M.; Ogami, A.; Ueda, K. *Chem. Mater.* **2003**, *15*, 1456.
9. Sinha Ray, S.; Okamoto, M. *J. Prog. Polym. Sci.* **2003**, *28*, 1539.
10. Denault, J.; Ton–That, M.T.; Bloch, J. 6th Annual SPE Automotive Composites Conference, Troy, MI, 2006. Available at http://www.speautomotive.com/SPEA_CD/SPEA2006/c.htm (accessed October, 2012).
11. Meng, Q. K.; Hetzer, M.; De Kee, D. J. *Compos. Mater.* **2011**, *45*, 1145.
12. Serizawa, S.; Inoue, K.; Iji, M. *J. Appl. Polym. Sci.* **2006**, *100*, 618.
13. Serizawa, S.; Inoue, K.; Iji, M. U.S. Pat 7445835 B2 (**2008**).
14. Ibrahim, N. A.; Yunus, W.; Othman, M.; Abdan, K. J. *Reinforc. Plast. Compos.* **2011**, *30*, 381.
15. Padwa, A. R. U.S. Pat 7,718,720B2, (**2010**).
16. Ahmad Thirmirzir, M. Z.; Mohd Ishak, Z. A.; Taib, R. M.; Rahim, S.; Mohamad Jani, S. J. *J. Appl. Polym. Sci.* **2011**, *122*, 3055.
17. Garcia, M.; Garmendia, I.; Garcia, J. J. *J. Appl. Polym. Sci.* **2008**, *107*, 2994.
18. Ochi, S. *Mech Mater* **2008**, *40*, 446.
19. Praprudivongs, C.; *Sombatsompop. N. Compos. B* **2012**, *43*, 2730.
20. Shi, Q. F.; Mou H. Y.; Gao L.; Yang J.; Guo W. H. *J. Polym. Environ.* **2010**, *18*, 567.
21. Sombatsompop, N.; Kositchaiyong, A.; Wimolmala E. *J. Appl. Polym. Sci.* **2006**, *102*, 1896.
22. Srebrenkoska, V.; Bogoeva Gaceva, G.; Dimeski, D. *Maced. J. Chem. Chem. Eng.* **2009**, *28*, 99.
23. Lee, B. H.; Kim, H. S.; Lee, S.; Kim, H. J.; Dorgan, J. R. *J. Compos. Sci. Tech.* **2009**, *69*, 2573.
24. Avella, M.; Bogoeva-Gaceva, G.; Buzarovska, A.; Errico, M. E.; Gentile, G.; Grozdanov, A. *J. Appl. Polym. Sci.* **2008**, *108*, 3542.
25. Bocchini, S.; Battegazzore, D.; Frache, A. *Carbohydr Polym.* **2010**, *82*, 802.
26. Nam, P. H.; Fujimori, A.; Masuko, T. *J. Appl. Polym. Sci.* **2004**, *93*, 2711.
27. Ishida, H. U.S. Pat 6,160,042, (**2000**).
28. Dai, B. Q.; Zhang, G. L. *Mater. Chem. Phys.* **2003**, *78*, 304.
29. Technical data sheet from Southern Clay Product, Inc. Available at http://www.scprod.com/product_bulletins/PB%20Cloisite%2030B.pdf (accessed October, 2012).
30. Technical data sheet from M K Impex Co. Ltd. Available at <http://lowerfriction.com/pdf/11.pdf> (accessed October, 2012).
31. Miles, I. S.; Rostami S. In *Multicomponent Polymer Systems*, 1st ed.; Longman Scientific & Technical: New York, **1992**.
32. Serizawa, S.; Inoue, K.; Iji, M. U.S. Pat 7,445,835 B2 (**2008**).
33. Liao, R.; Yang, B.; Yu, W.; Zhou, C. *J. Appl. Polym. Sci.* **2007**, *104*, 310.